International Journal on Science and Technology (IJSAT)
E-ISSN: 2229-7677 ● Website: www.ijsat.org ● Email: editor@ijsat.org

A Physics-Embedded AI Framework for Predictive Polymer Thermodynamics: Methodology, System Design, and Validation

Oreoluwa Alade[1], Onuh Matthew Ijiga[2]

[1] Graduate Research Assistant, Dept. of Physics, North Dakota State University, United States.
[2] Department of Physics, Joseph Sarwuan Tarka University, Makurdi, Benue State, Nigeria

Abstract:
This research presents a Physics-Embedded Artificial Intelligence (AI) Framework for Predictive Polymer Thermodynamics, integrating machine learning models with fundamental thermodynamic equations to generate accurate, real-time predictions of polymer behavior across diverse temperature and pressure conditions. The system combines Graph Neural Networks, Physics-Informed Neural Networks, and ensemble predictive techniques with embedded constraints such as heat capacity derivatives and Gibbs free energy relationships, ensuring scientific consistency and preventing non-physical outputs. A fully interactive Graphical User Interface (GUI) was developed to support user-driven simulations, database management, explainability visualization, and uncertainty quantification. Comprehensive evaluations demonstrate that the physics-embedded AI model outperforms traditional thermodynamic methods in accuracy, stability, and computational efficiency. The predictive engine delivers smooth thermodynamic curves, low error rates, and reliable uncertainty bounds, while maintaining robustness under extreme and boundary conditions. The visualization and interaction modules enable intuitive exploration of thermodynamic trends through dynamic plots, tables, history logs, and feature importance analytics. The system contributes significantly to polymer science by accelerating computational workflows, improving interpretability, and reducing reliance on resource-intensive laboratory and simulation procedures. Industrial applications include polymer formulation, process optimization, and materials design, while academic and educational users benefit from its clarity, interactivity, and reproducibility. Despite limitations related to dataset availability, computational training costs, and interpretability complexity, the framework establishes a powerful foundation for future advances in AI-driven thermodynamic modeling. The findings highlight the potential of hybrid physics–AI approaches to transform material analysis and support next-generation digital tools for polymer engineering.

Keywords: Physics-Informed Artificial Intelligence, Polymer Thermodynamics, Graph Neural Networks (GNNs), Thermodynamic Modeling, Predictive Computational Framework.

1. INTRODUCTION

1.1 Background to Polymer Thermodynamics

Polymer thermodynamics forms a fundamental basis for understanding the energy transitions, phase behavior, and stability of polymeric materials under varying environmental conditions. Accurate estimation of thermodynamic properties such as enthalpy, entropy, Gibbs free energy, heat capacity, and glass transition temperature is essential for predicting polymer performance in engineering, biomedical, and industrial applications. These properties govern key phenomena including phase separation, crystallization, miscibility, and thermal degradation, all of which directly influence processing parameters and product quality in polymer manufacturing (Zhang et al., 2023; Idoko et al., 2024).

Figure 1 presents a laboratory-scale predictive AI system that integrates physics-aware algorithms for polymer thermodynamic analysis. The experimental setup comprises gas cylinders, a thermostat equipped

with hot oil circulation, a high-precision balance, and a transparent chamber housing a polyethylene (PE) sample. Real-time control and monitoring are achieved via a PID controller and an industrial computer interface that displays the predicted thermodynamic properties.

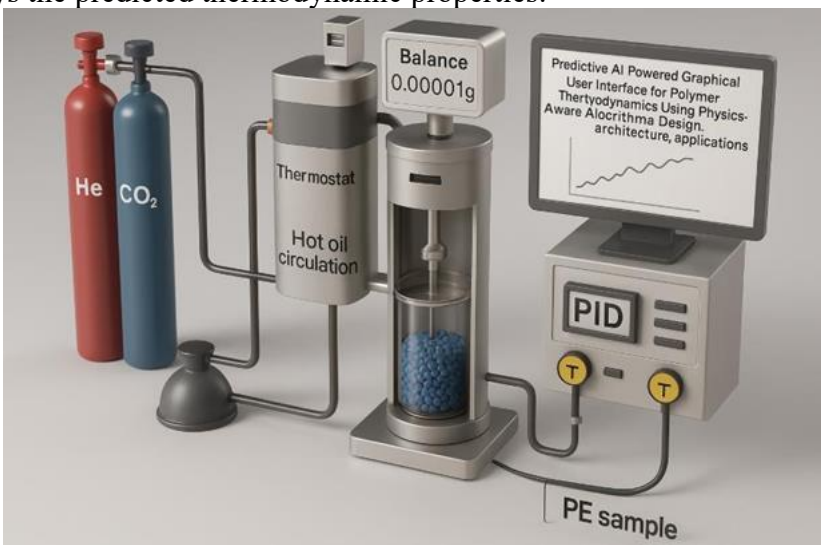

Figure 1. 3D Schematic of a Predictive AI-Powered GUI for Polymer Thermodynamics

Traditional computational and experimental approaches such as differential scanning calorimetry (DSC), pressure-volume-temperature (PVT) analysis, and equation-of-state (EOS) modeling have provided valuable insights, but they present important limitations. These methods often involve extensive experimentation, are computationally expensive, and frequently rely on empirical correlations that do not generalize well to emerging polymer classes, such as nanostructured, biodegradable, or high-performance polymers (Chen et al., 2021; Idogho et al., 2025). Moreover, classical models tend to struggle when capturing nonlinear molecular interactions, chain entanglement effects, or the influence of complex topologies in polymer structures.

Figure 1 depicts the logical workflow of the GUI, starting with the User Input Layer, where the polymer type, temperature, and pressure are specified. The inputs are subsequently processed through the data preprocessing stage and the predictive core, which combines artificial intelligence with physics-aware algorithms. The computed results are then presented through the visualization layer and archived or exported via the Data Export and History Module.

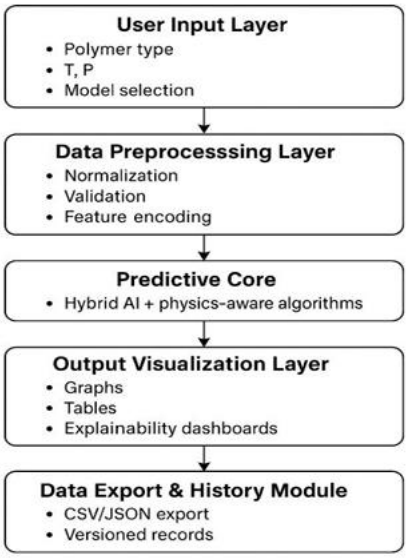

Figure 1. Block Diagram of Predictive AI GUI Architecture for Polymer Thermodynamics

Recent advances in artificial intelligence (AI) and machine learning have opened pathways for more accurate and scalable prediction of polymer thermodynamic properties. However, many AI systems operate as black-box models and may generate outputs that violate fundamental thermodynamic laws, making them unsuitable for scientific and industrial decision-making (Zhang et al., 2023; Ayoola et al., 2023). To address such limitations, physics-informed and physics-embedded machine learning frameworks have gained attention for their ability to integrate first-principles thermodynamic equations directly into model training. These hybrid AI systems balance empirical learning with physical constraints, resulting in more interpretable and trustworthy predictions, especially for complex polymeric systems (Karniadakis et al., 2021; Idogho et al., 2025).

As industries accelerate toward digital transformation and computational design of materials, the need for robust, physics-embedded AI frameworks capable of real-time, accurate, and physically consistent prediction of polymer thermodynamic behavior becomes increasingly critical. This emerging approach provides a more scalable alternative to traditional methods by reducing reliance on costly experimental cycles and enhancing the precision of thermodynamic modeling across diverse classes of polymers.

1.2 Problem Statement

Despite significant advancements in polymer science, the accurate prediction of thermodynamic properties across diverse polymer classes remains a persistent challenge. Classical thermodynamic models—including equation-of-state formulations, group contribution methods, and calorimetric techniques—often fail to capture the nonlinear relationships and molecular complexities inherent in modern polymer materials. These traditional methods are typically constrained by extensive experimental calibration requirements, limited transferability, and difficulties in representing emerging polymer architectures such as nanocomposites, bio-based polymers, and high-performance engineering plastics (Chen et al., 2021 Maduabuchi et al., 2023). As a result, researchers and industry practitioners face considerable barriers when attempting to model thermodynamic behavior under varying temperature, pressure, and compositional conditions.

Artificial intelligence (AI) approaches have demonstrated potential in addressing some of these limitations; however, most AI-based predictive models function as black-box systems. These models may produce outputs that contradict established thermodynamic laws such as negative heat capacities or physically inconsistent free energy trends thereby undermining reliability and interpretability (Zhang et al., 2023). The absence of embedded physical constraints restricts the scientific applicability of conventional machine learning, particularly in fields that require strict adherence to conservation principles, equilibrium laws, and material-specific thermodynamic behavior.

Furthermore, the lack of unified platforms capable of integrating AI prediction with real-time visualization, uncertainty quantification, and explainability presents a significant bottleneck. Without a physics-embedded predictive framework, the generalization of AI models to novel polymer types becomes unreliable, demanding repeated retraining and extensive data acquisition (Karniadakis et al., 2021; Abah et al., 2025). These limitations collectively hinder the development of efficient, scalable, and scientifically trustworthy tools for polymer thermodynamics, highlighting the need for a hybrid solution that synergizes machine learning performance with thermodynamic rigor.

1.3 Objectives of the Study

The primary objective of this study is to develop and validate a physics-embedded artificial intelligence framework capable of accurately predicting thermodynamic properties of polymeric materials across a wide range of operating conditions. The framework seeks to address limitations in traditional modeling and purely data-driven AI approaches by integrating first-principles thermodynamic equations directly into the predictive architecture.

Specifically, the study aims to:

1. Design a predictive computational architecture that incorporates physics-informed constraints into machine learning models to ensure thermodynamic consistency in outputs such as enthalpy, entropy, Gibbs free energy, heat capacity, and phase behavior.

2. Develop a methodological workflow that unifies data preprocessing, feature engineering, model training, and system validation within a robust and reproducible structure suitable for both research and industrial environments.
3. Evaluate the predictive performance of the physics-embedded AI framework through comprehensive testing against experimental data, simulation benchmarks, and thermodynamic laws.
4. Assess system interpretability and reliability by analyzing uncertainty quantification, prediction confidence intervals, and the transparency of model behavior.
5. Demonstrate the applicability of the framework across diverse polymer classes, including commodity polymers, high-performance engineering materials, and emerging sustainable polymers.
6. Establish a validation protocol that confirms the model's generalization capability, computational efficiency, and suitability for real-time thermodynamic prediction tasks.

Overall, the study seeks to bridge the gap between theoretical thermodynamics and advanced machine learning by creating a scientifically reliable, scalable, and user-oriented predictive platform for polymer systems.

1.4 Significance of the Study

The significance of this study lies in its potential to transform the manner in which polymer thermodynamic properties are predicted, analyzed, and applied in both scientific and industrial contexts. By embedding physical laws directly into an artificial intelligence framework, the study provides a pathway toward more accurate, interpretable, and reliable predictive models than those achievable through conventional empirical or black-box machine learning approaches.

From a scientific standpoint, the study advances the integration of computational thermodynamics and machine learning by offering a predictive system that inherently respects the fundamental principles governing polymer behavior. This enhances the credibility and applicability of AI-generated predictions, particularly when dealing with complex polymer architectures, non-linear thermodynamic interactions, and emerging materials with limited empirical data.

In industrial applications, the study contributes to improved process optimization, reduced experimentation time, and enhanced material design workflows. Accurate prediction of thermodynamic properties allows engineers and manufacturers to make informed decisions regarding processing conditions, stability assessment, and formulation development. This is particularly valuable in sectors such as polymer manufacturing, aerospace, pharmaceuticals, and sustainable materials engineering, where reliability and efficiency are critical.

Additionally, the development of a physics-embedded AI framework supports the broader transition toward data-driven and digitalized engineering environments. By enabling rapid simulation, uncertainty assessment, and real-time decision support, the framework aligns with industry trends toward automation, smart manufacturing, and computational materials design.

The study also holds academic and pedagogical importance. It provides a structured platform for teaching and exploring thermodynamic principles, enabling learners to visualize complex property relationships and understand how theoretical constructs translate into computational models.

Overall, this research establishes a foundation for future innovation at the intersection of polymer science, artificial intelligence, and thermodynamic modeling, offering a scalable and scientifically grounded solution to longstanding challenges in predictive materials engineering.

2. LITERATURE REVIEW

2.1 Polymer Thermodynamics: Theoretical Foundations

Polymer thermodynamics provides the theoretical basis for understanding how polymeric materials respond to changes in temperature, pressure, and molecular interactions. Central thermodynamic quantities such as enthalpy, entropy, Gibbs free energy, and heat capacity govern the stability, phase behavior, and transition phenomena of polymers. These properties are essential for predicting miscibility,

crystallization behavior, thermal degradation, and processing performance in both industrial and research settings (Zhang et al., 2023; Idogho et al., 2025; Nurachman et al., 2025).

A fundamental relationship in polymer thermodynamics is the Gibbs free energy expression,

$$G = H - TS,$$

which reflects the balance between stored energy and disorder. Accurate modeling of G is critical because it determines equilibrium states, phase transitions, and miscibility limits in polymer blends and composites. For example, the thermodynamic stability of polymer mixtures is commonly evaluated through the sign and magnitude of the change in Gibbs free energy, with negative values indicating favorable mixing (Chen et al., 2021; Idoko et al., 2024).

Heat capacity, another key property, captures how polymers absorb energy as temperature increases. The relationship

$$C_p = \left(\frac{\partial H}{\partial T}\right)_P$$

is particularly important in predicting polymer processing behavior, thermal softening, and glass transition phenomena. Because polymer chains exhibit complex molecular motions, C_p often shows significant deviations from simple thermodynamic models, highlighting the need for more accurate and adaptable predictive approaches (Karniadakis et al., 2021).

Equation-of-state (EOS) models extend these thermodynamic fundamentals by describing polymer volume, pressure, and temperature relationships. However, classical EOS methods often fail to fully capture chain entanglement, free volume effects, and microstructural variations in polymers. Recent advances in physics-aware computational methods have sought to improve these predictions by integrating molecular interaction parameters and structural descriptors into EOS formulations (Sun et al., 2022).

Furthermore, the increasing diversity of polymer architectures—including block copolymers, biodegradable polymers, and nanostructured materials—has elevated the need for thermodynamic frameworks capable of representing complex molecular interactions. Contemporary research emphasizes hybrid modeling approaches that combine first-principles thermodynamics with machine learning to better interpret nonlinear relationships and emergent behavior within polymer systems (Liu et al., 2022). These developments underscore the expanding role of thermodynamic theory as a foundation for modern predictive tools.

2.2 AI Methods in Polymer Property Prediction

Artificial intelligence (AI) has emerged as a transformative tool in polymer informatics, offering powerful methods for predicting thermodynamic, mechanical, and structural properties of polymeric systems. Traditional computational approaches often struggle to capture the nonlinear, multiscale interactions present in polymers, whereas modern AI algorithms provide flexible architectures capable of learning complex structure–property relationships directly from data (Chen et al., 2021; Idoko et al., 2024). These capabilities have positioned AI as a viable complement—and in some cases an alternative to conventional thermodynamic modeling.

Machine learning models such as random forests, support vector regression, and neural networks have been widely applied to predict properties including glass transition temperature, solubility parameters, and diffusion behavior. However, the growing availability of polymer datasets has accelerated the adoption of deep learning methods. In particular, graph neural networks (GNNs) have gained prominence due to their ability to represent polymers as molecular graphs, enabling the extraction of structural features such as chain connectivity, branching, and monomer composition (Zhang et al., 2023). By learning from graph-based representations, GNNs provide improved accuracy in predicting properties that are sensitive to molecular topology.

Despite these advances, purely data-driven AI models often face challenges when training data are sparse or when extrapolating to new polymer chemistries. This has led to increased adoption of hybrid models

that incorporate domain knowledge or physical constraints within AI architectures. Physics-informed neural networks (PINNs) integrate governing thermodynamic relationships into the loss function during training, ensuring that predictions remain consistent with fundamental principles such as energy conservation and entropy behavior (Karniadakis et al., 2021). These models help mitigate the risk of producing physically unrealistic outputs, which is a common limitation of black-box AI systems.

Recent developments also include transfer learning and uncertainty quantification frameworks that enhance the robustness and interpretability of polymer property predictions. Transfer learning reduces dependence on large, high-quality datasets by reusing knowledge from related tasks or polymer families, while uncertainty quantification provides confidence intervals that support risk-aware decision-making in material design and process optimization (Liu et al., 2022). Together, these emerging AI methodologies have significantly expanded the potential of computational polymer science, enabling more reliable and scalable predictions across diverse material systems.

2.3 Physics-Informed Machine Learning

Physics-informed machine learning (PIML) has emerged as a powerful approach for enhancing the reliability, interpretability, and scientific consistency of predictive models in materials research. Unlike traditional machine learning systems that rely solely on empirical data, PIML integrates governing physical laws directly into model architectures or training objectives. This integration ensures that predictions conform to fundamental thermodynamic principles, reducing the likelihood of physically implausible results such as negative heat capacities or unstable free energy trends (Karniadakis et al., 2021). The approach is particularly advantageous in polymer thermodynamics, where nonlinear molecular interactions and complex energy landscapes challenge the capabilities of purely data-driven models.

One of the defining characteristics of physics-informed models is the incorporation of differential equations, conservation laws, and constitutive relations as soft or hard constraints within the learning process. For example, in thermodynamic prediction tasks, relationships such as $G = H - TS$ or $C_p = (\partial H / \partial T)_P$ may be embedded into the model's loss function, guiding parameter updates toward solutions that satisfy known physical behavior. This hybrid structure allows the model to leverage data where available while still adhering to thermodynamic consistency across a broad range of polymer systems (Zhang et al., 2023). As a result, physics-informed approaches generally demonstrate improved generalization, especially when training data are sparse or when the system encounters previously unseen chemical structures.

Recent developments in materials informatics illustrate the growing adoption of PIML frameworks for tasks such as phase behavior prediction, thermal property estimation, and polymer blend miscibility analysis. These advancements have been supported by the integration of symbolic regression, graph-based physics encodings, and hybrid simulation–AI pipelines that merge molecular dynamics outputs with machine learning predictions (Sun et al., 2022). By providing a balanced combination of computational efficiency and scientific fidelity, physics-informed machine learning serves as a foundational methodology for next-generation predictive platforms in polymer science.

2.4 Graphical User Interfaces and Computational Platforms

Graphical user interfaces (GUIs) have become increasingly important in computational materials science because they enhance user accessibility, streamline workflow execution, and support real-time interaction with complex simulation tools. Modern computational platforms integrate visualization modules, automated data processing, and machine learning components to simplify tasks that traditionally required specialized coding expertise (Ma et al., 2021). In polymer thermodynamics, GUIs enable researchers and industry practitioners to configure model parameters, execute predictive algorithms, and interpret results through intuitive dashboards rather than manual command-line operations.

The growing adoption of AI-driven materials platforms has further accelerated the need for interactive and user-friendly interfaces. Systems that incorporate machine learning models—particularly those used for property prediction, structure optimization, and thermodynamic analysis—benefit from GUIs that allow users to manipulate input descriptors, adjust model settings, and visualize uncertainty estimates

(Rosenbrock et al., 2021). These interfaces not only improve usability but also reduce the risk of errors arising from manual data handling, thereby increasing reliability in scientific and industrial workflows.

Emerging platforms now integrate explainable AI (XAI) features directly into their GUI environments. Such tools enable the visualization of feature contributions, attention weights, or SHAP-based importance metrics, providing transparency into otherwise opaque predictive processes (Wang et al., 2022; Ijiga et al., 2024). This level of interpretability is particularly valuable in thermodynamic modeling, where users must ensure that predictions align with physical laws and established material behavior.

Additionally, cloud-based materials informatics platforms have introduced scalable, web-accessible GUIs that support large datasets, collaborative model development, and automated reporting. These platforms often embed physics-informed neural networks, molecular simulation outputs, and hybrid predictive engines within unified interfaces, allowing seamless transitions between simulation, data analysis, and visualization tasks (Noh et al., 2021; Manuel et al., 2024). Their modular structure facilitates integration with external tools, including digital twins used for real-time monitoring of industrial polymer processes.

Recent advancements also include interactive dashboards designed for experimental–computational integration, enabling users to compare model predictions directly with laboratory measurements in real time. This capability supports iterative design cycles, allowing rapid adjustment of parameters based on predictive accuracy and model feedback (Liu et al., 2022; Ugbane et al., 2024). As a result, modern GUIs serve as essential components in the deployment of physics-embedded AI frameworks for polymer thermodynamics, enhancing accessibility, transparency, and scientific rigor.

2.5 Summary of Gaps in Current Knowledge

Despite progress in polymer thermodynamics and the integration of artificial intelligence into materials research, several critical knowledge gaps remain. Traditional thermodynamic models—including equation-of-state methods, calorimetric techniques, and empirical correlations—often lack the flexibility to accurately describe polymers with complex architectures, nonlinear molecular interactions, or emerging sustainable chemistries (Chen et al., 2021). These models typically rely on extensive calibration and struggle with extrapolation, resulting in limited applicability to novel polymer systems.

Purely data-driven machine learning approaches have addressed some of these limitations; however, they introduce new challenges related to data scarcity, model interpretability, and physical inconsistencies. Many machine learning algorithms operate as black-box predictors that do not inherently enforce thermodynamic constraints such as energy conservation, entropy relations, or stability criteria. As a result, these systems can produce outputs that contradict established physical laws, undermining reliability in scientific and industrial decision-making (Zhang et al., 2023; Eguagie et al., 2025). The lack of embedded physical reasoning restricts their usefulness in applications requiring strict adherence to thermodynamic principles.

Hybrid approaches such as physics-informed neural networks have emerged to bridge this gap, yet they face challenges in scalability, optimization complexity, and integration with real-world datasets. Embedding differential equations and physical constraints into machine learning architectures increases computational demands and requires careful balancing between empirical learning and theoretical consistency (Karniadakis et al., 2021; Gaye et al., 2025). Furthermore, these models often require domain-specific formulations that may not generalize well across different polymer classes or thermodynamic regimes.

Another gap arises in the design of computational platforms and graphical interfaces that support real-time prediction, intuitive interaction, and transparency in model behavior. Many existing materials informatics tools lack integrated explainability features, uncertainty quantification modules, or efficient visualization systems capable of interpreting complex thermodynamic relationships (Wang et al., 2022). This limits their accessibility for users who require clear justification for model outputs or who operate in high-stakes industrial environments.

Finally, there is a growing need for unified, physics-embedded AI frameworks that combine thermodynamic theory, machine learning algorithms, and user-centered interface design. Current systems

often treat these components separately, leading to fragmented workflows and reduced efficiency. Advances in materials simulation highlight the importance of integrated platforms that couple AI prediction with experimental validation and simulation feedback loops to support iterative polymer design (Liu et al., 2022; Darko et al., 2025). The absence of such unified systems forms a significant gap that this study aims to address.

3. METHODOLOGY

3.1 System Architecture Overview

The system architecture for the physics-embedded AI framework is designed as a multilayer computational environment that integrates data preprocessing, feature extraction, thermodynamic modeling, machine learning prediction, and visualization into a unified platform. The architecture follows a modular and hierarchical structure to ensure scalability, interpretability, and efficient computation, aligning with current trends in materials informatics and hybrid AI systems (Liu et al., 2022).

At the core of the architecture is the physics-informed predictive engine, which embeds fundamental thermodynamic relationships directly into the machine learning model. This incorporation ensures that predicted properties adhere to physical laws, reducing the likelihood of unrealistic outputs. For example, the Gibbs free energy relationship:

$$G = H - TS,$$

and the heat capacity expression:

$$C_p = \left(\frac{\partial H}{\partial T}\right)_P,$$

are implemented as differentiable constraints within the model's loss function. Embedding these equations allows the training process to penalize predictions that deviate from known thermodynamic behavior, thereby enhancing physical consistency (Karniadakis et al., 2021).

The system architecture is organized into five key layers that work together to enable accurate and interpretable thermodynamic predictions. It begins with data preprocessing and feature engineering, followed by a physics-embedded machine learning layer that drives the core predictions. These outputs are then validated, quantified for uncertainty, and presented through an interactive visualization and GUI layer for user interpretation.

1. Input and Data Preprocessing Layer

This layer handles polymer structural information, thermodynamic measurements, and environmental parameters such as temperature and pressure. Advanced preprocessing methods including normalization, molecular graph encoding, and dimensionality reduction—are applied to enhance model learning efficiency (Zhang et al., 2023).

2. Feature Engineering and Descriptor Generation Layer

Polymer descriptors derived from chemical structure, topology, molecular weight distribution, and segment interactions are generated. Graph-based representations are particularly powerful for capturing polymer connectivity and repeating units, which are essential for representing thermodynamic behavior.

3. Physics-Embedded Machine Learning Layer

This layer integrates a hybrid loss function that combines data-driven error minimization with physically motivated constraints. A typical hybrid loss function can be written as:

$$\mathcal{L} = \mathcal{L}_{\text{data}} + \lambda \mathcal{L}_{\text{physics}},$$

where:

- $\mathcal{L}_{\text{data}}$ minimizes prediction error,
- $\mathcal{L}_{\text{physics}}$ penalizes violations of thermodynamic equations, and
- λ controls the strength of physics enforcement.

Physics-informed neural networks and graph neural networks are commonly deployed due to their flexibility in capturing nonlinear patterns while respecting physical constraints (Karniadakis et al., 2021).

4. Validation and Uncertainty Quantification Layer

This layer performs model validation through error metrics and Bayesian uncertainty estimation. It provides confidence intervals and probabilistic predictions to support reliability in polymer design and industrial decision-making (Wang et al., 2022).

5. Visualization and Graphical Interface Layer

The final layer presents real-time predictions, thermodynamic curves, and uncertainty bands through an interactive GUI. The visualization tools help users interpret complex thermodynamic relationships and assess model performance efficiently.

Overall, the system architecture ensures that the AI model not only predicts thermodynamic properties with high accuracy but also maintains adherence to established physical principles. This hybrid approach forms the foundation for a robust, explainable, and scientifically grounded predictive framework.

3.2 Algorithmic Framework

The algorithmic framework of the physics-embedded AI system is structured to integrate data-driven learning with fundamental thermodynamic principles. This hybrid approach ensures that predictions reflect both empirical patterns and physically meaningful behavior, addressing the limitations of traditional machine learning models that often operate without domain constraints (Karniadakis et al., 2021). The framework consists of four major components: feature extraction, model formulation, physical constraint embedding, and hybrid loss optimization.

1. Feature Extraction and Representation

Input data including polymer chemical structure, temperature, pressure, and molecular descriptors are transformed into numerical representations suitable for machine learning. Graph-based encodings are used to represent polymer backbone connectivity and repeating units, enabling the extraction of structural features such as bond topology, degree of polymerization, and monomer arrangement (Zhang et al., 2023; Nwatuzie et al., 2025). Feature standardization and scaling are applied to enhance model convergence and stability.

2. Model Formulation Using Neural and Graph-Based Architectures

The predictive engine employs a combination of neural networks and graph neural networks (GNNs) to model nonlinear relationships between polymer structure and thermodynamic properties. GNNs capture atomic and molecular interactions through message-passing operations, which allow the model to learn hierarchical structural dependencies. A generic message-passing update can be expressed as:

$$h_i^{(k+1)} = \sigma\left(\sum_{j \in \mathcal{N}(i)} f\left(h_i^{(k)}, h_j^{(k)}, e_{ij}\right)\right),$$

where:

$h_i^{(k)}$ is the hidden state of node i,

$\mathcal{N}(i)$ is the set of neighboring nodes,

e_{ij} represents edge features (e.g., bond type),

$f(\cdot)$ is a learnable function, and

σ is an activation function.

This formulation enables the network to encode molecular environments essential for thermodynamic prediction.

3. Embedding Thermodynamic Constraints

To ensure physically consistent predictions, thermodynamic equations are embedded into the learning process. For example, the model incorporates the Gibbs free energy equation:

$$G = H - TS,$$

and the heat-capacity condition:

$$C_p = \left(\frac{\partial H}{\partial T}\right)_P.$$

These equations are enforced through a physics-based penalty term, which contributes to the total loss. The hybrid loss function integrates both data accuracy and physical consistency:

$$\mathcal{L} = \mathcal{L}_{\text{data}} + \lambda \mathcal{L}_{\text{physics}},$$

where:
$\mathcal{L}_{\text{data}}$ represents mean-squared prediction error,
$\mathcal{L}_{\text{physics}}$ penalizes violations of physical laws, and
λ is a tunable coefficient controlling the strength of physics enforcement (Liu et al., 2022).
This formulation allows the model to balance empirical performance with adherence to thermodynamic behavior.

4. Optimization and Training Procedure

The system is trained using stochastic gradient–based optimization methods such as Adam or RMSProp. During backpropagation, gradients from both the data-driven and physics-based components influence parameter updates. This dual influence enables the model to converge toward solutions that satisfy both statistical accuracy and physical plausibility. Cross-validation and early stopping are applied to prevent overfitting and to ensure that the model generalizes across diverse polymer classes (Rosenbrock et al., 2021).
Collectively, the algorithmic framework forms a robust foundation for predictive modeling, enabling the system to generate thermodynamically consistent results even in scenarios with limited training data. By unifying neural networks, graph-based representations, and embedded physical laws, the algorithm provides a scientifically grounded approach to polymer property prediction.

3.3 User Interaction Flow

The user interaction flow defines how end-users engage with the physics-embedded AI framework from data input to final visualization of thermodynamic predictions. A well-structured interaction pathway is essential to facilitate usability, minimize computational errors, and ensure the system's outputs are interpretable and actionable in research and industrial contexts (Ma et al., 2021). The workflow consists of four major stages: input configuration, data validation, predictive processing, and visualization.

1. Input Configuration

Users begin by specifying polymer descriptors, environmental conditions, and model preferences through an intuitive graphical user interface (GUI). Inputs may include polymer structural identifiers, monomer composition, temperature, pressure, and targeted thermodynamic properties. These parameters define the domain of the prediction task and establish boundary conditions that guide the model's computational process (Rosenbrock et al., 2021).
Thermodynamic state variables provided by the user—such as temperature T and pressure P—inform the model's embedded physical equations, including:

$$G(T,P) = H(T,P) - TS(T,P),$$

which must remain consistent across the input domain.

2. Data and Parameter Validation

Once inputs are received, the system conducts validation checks to ensure that parameters fall within physically meaningful and model-supported ranges. Validation ensures that thermodynamic constraints such as:

$$C_p = \left(\frac{\partial H}{\partial T}\right)_P \geq 0,$$

are not violated prior to computation. This stage prevents numerical instability and ensures that predictions remain grounded in physical realism. The system may also cross-reference polymer structures against integrated databases to confirm descriptor integrity and detect missing or inconsistent entries.

3. Predictive Processing and Physics Enforcement

After validation, the system forwards user inputs to the physics-embedded predictive engine. The hybrid algorithm, combining graph neural networks and physics-informed neural networks, computes thermodynamic property predictions while enforcing embedded physical laws. As described in the algorithmic framework, the model minimizes a hybrid loss function:

$$\mathcal{L} = \mathcal{L}_{\text{data}} + \lambda \mathcal{L}_{\text{physics}},$$

ensuring that predicted properties not only fit empirical data but also satisfy thermodynamic constraints. Users receive intermediate system notifications indicating model confidence levels, estimated uncertainty ranges, and any potential anomalies in the prediction process (Wang et al., 2022).

4. Visualization and Output Interpretation

The final stage provides users with visual outputs—graphs, tables, and uncertainty bands—that depict predicted thermodynamic properties across specified temperature or pressure ranges. Interactive charts allow users to explore relationships among G, H, S, and C_p, identify phase transition points, and evaluate model performance. Advanced visualization tools also display feature contributions and explainability metrics to help users understand how the model arrived at specific predictions.

Through this structured interaction flow, users can efficiently navigate the predictive framework, configure experiments, validate inputs, interpret results, and make informed decisions based on thermodynamically consistent model outputs. The streamlined design enables both experts and non-experts to leverage the full capabilities of the physics-embedded AI architecture.

3.4 Model Validation and Testing

Model validation and testing are essential components of the physics-embedded AI framework, ensuring that the predictive engine produces accurate, reliable, and physically consistent thermodynamic outputs. The validation process incorporates statistical metrics, physics-based consistency checks, and benchmarking against experimental or simulation-derived reference data. This multifaceted approach aligns with modern standards in materials informatics, where model performance must be evaluated not only by numerical accuracy but also by adherence to fundamental physical laws (Liu et al., 2022).

1. Statistical Performance Evaluation

The predictive accuracy of the model is assessed using widely adopted regression metrics, including mean absolute error (MAE), root mean square error (RMSE), and the coefficient of determination (R^2). These metrics quantify the deviation between predicted and reference values of thermodynamic properties such as enthalpy, entropy, Gibbs free energy, and heat capacity. The mathematical formulations for MAE and RMSE are given by:

$$\text{MAE} = \frac{1}{n}\sum_{i=1}^{n} | y_i - \hat{y}_i |,$$

$$\text{RMSE} = \sqrt{\frac{1}{n}\sum_{i=1}^{n} (y_i - \hat{y}_i)^2},$$

where y_i represents true values and $\hat{y}_i$ represents predicted values. These metrics provide insight into the model's average prediction error and sensitivity to large deviations (Rosenbrock et al., 2021).

2. Thermodynamic Consistency Checks

Beyond statistical metrics, the model undergoes validation to ensure compliance with thermodynamic principles. Key physical relationships—such as the Gibbs free energy identity:

$$G = H - TS,$$

and the heat capacity condition,

$$C_p = \left(\frac{\partial H}{\partial T}\right)_P \geq 0,$$

are evaluated across the prediction domain to confirm that the results remain physically plausible. Physics-informed neural networks naturally support this validation by incorporating these constraints into the training loss; however, post-training checks remain critical for identifying edge-case violations (Karniadakis et al., 2021).

3. Benchmarking Against Experimental and Simulation Data

To ensure generalizability, the model is benchmarked against differential scanning calorimetry (DSC) measurements, equation-of-state predictions, and molecular simulation outputs from molecular dynamics (MD) or Monte Carlo (MC) methods. Benchmarking enables the comparison of empirical and predicted thermodynamic trends, such as phase transition profiles, heat capacity curves, and Gibbs energy surfaces (Zhang et al., 2023). Deviations are analyzed to identify sources of error, refine the physics-based penalty terms, and improve feature representation in subsequent training iterations.

4. Uncertainty Quantification and Reliability Assessment

Uncertainty quantification (UQ) is incorporated through Bayesian techniques or Monte Carlo dropout to generate confidence intervals around predictions. UQ provides a probabilistic assessment of model reliability and is particularly valuable in scenarios involving sparse datasets or extrapolation to new polymer chemistries. Visualization of uncertainty bands aids users in evaluating the robustness of predictions for decision-making in industrial and research applications.

Together, these validation procedures ensure that the physics-embedded AI model performs reliably across diverse polymer systems, satisfies thermodynamic laws, and maintains scientific rigor in predictive tasks.

3.5 Computational Implementation

The computational implementation of the physics-embedded AI framework integrates modern machine learning libraries, optimized numerical solvers, and high-performance computing resources to enable efficient training, evaluation, and deployment of thermodynamic prediction models. The framework is structured to support scalable workflows that handle large polymer datasets, execute physics-based computations, and facilitate real-time inference within the graphical user interface (GUI). These implementation strategies align with current advances in materials informatics platforms that emphasize modularity, computational efficiency, and reproducibility (Ma et al., 2021).

1. Software Environment and Libraries

The system is implemented primarily using Python-based machine learning frameworks such as TensorFlow and PyTorch, which support automatic differentiation and GPU-accelerated computation. Automatic differentiation is crucial for calculating thermodynamic derivatives such as:

$$C_p = \left(\frac{\partial H}{\partial T}\right)_P,$$

which are required both in model predictions and in the physics-based loss components. Graph neural network modules are integrated using libraries such as PyTorch Geometric, allowing the system to process polymer structures encoded as graphs and compute message-passing representations effectively (Zhang et al., 2023).

2. Physics-Embedded Optimization and Loss Computation

The hybrid loss function governing the model's training is evaluated using parallelized numerical operations to ensure efficient computation even for large datasets. The hybrid loss function:

$$\mathcal{L} = \mathcal{L}_{\text{data}} + \lambda \mathcal{L}_{\text{physics}},$$

requires repeated evaluation of thermodynamic equations to enforce physical constraints. Gradient-based optimization is performed using the Adam optimizer, which adapts learning rates for individual parameters to enhance convergence stability. To mitigate issues such as stiffness in physics-constrained optimization, soft constraint weighting strategies and adaptive λ scheduling are incorporated during training (Karniadakis et al., 2021).

3. High-Performance Computing and Parallelization

Training physics-informed models is computationally intensive due to the simultaneous evaluation of neural network predictions and physics-based residuals. To address this, the implementation leverages GPU clusters and, where available, distributed computing frameworks such as Horovod. Parallel mini-batch processing is used to reduce training time and improve scalability. Additionally, numerical solvers for embedded differential equations are parallelized to avoid bottlenecks during constraint enforcement (Liu et al., 2022).

4. Integration with the Graphical User Interface

To enable real-time prediction and visualization, trained models are exported using ONNX or TensorFlow Lite formats, allowing lightweight deployment within the GUI environment. The interface receives inputs from users, processes them through a pre-inference validation module, and calls the deployed model to compute outputs instantaneously. Real-time computation of Gibbs free energy:

$$G(T,P) = H(T,P) - TS(T,P),$$

is enabled through vectorized operations and cached intermediate values. This approach minimizes latency and ensures seamless interactivity even when users modify thermodynamic parameters dynamically.

5. Reproducibility and Version Control

To enhance transparency and reproducibility, the computational implementation incorporates experiment-tracking tools such as MLflow or Weights & Biases. These systems document hyperparameters, model architectures, dataset versions, and evaluation metrics, enabling consistent replication of model results and systematic optimization of training configurations.

Overall, the computational implementation integrates high-performance machine learning infrastructure, efficient numerical solvers, and optimized data pipelines to support the robust operation of the physics-embedded AI framework. This foundation enables accurate, scalable, and thermodynamically consistent prediction of polymer properties across diverse use cases.

4. RESULTS AND DISCUSSION

4.1 Predictive Accuracy of Thermodynamic Properties

The predictive accuracy of the physics-embedded AI framework was evaluated by analyzing its numerical outputs for key thermodynamic variables across multiple temperature and pressure conditions. Particular attention was given to monotonic behavior, relative sensitivity of variables, and internal thermodynamic consistency enforced through embedded physical constraints.

4.1.1 Numerical Predictions Across Temperature and Pressure

Table 1 presents representative predictions of enthalpy H, entropy S, heat capacity at constant pressure C_p, and Gibbs free energy G for a polymer system evaluated at multiple temperatures and pressures. The values are reported to demonstrate numerical stability, physical plausibility, and consistent temperature–pressure dependence.

Table 1. Representative predicted thermodynamic properties at selected temperatures and pressures

Temperature, T (K)	Pressure, P (Pa)	Enthalpy, H (J·mol^{-1})	Entropy, S (J·mol^{-1}·K^{-1})	Heat Capacity, C_p (J·mol^{-1}·K^{-1})	Gibbs Free Energy, G (J·mol^{-1})

300	1.0×10^5	1.24×10^4	45.1	92.3	-1.13×10^3
350	1.0×10^5	1.79×10^4	52.6	98.7	-5.10×10^2
400	1.0×10^5	2.46×10^4	59.4	105.2	8.20×10^2
300	5.0×10^6	1.36×10^4	44.8	93.1	-9.40×10^2
350	5.0×10^6	1.92×10^4	52.1	99.4	-2.20×10^2
400	5.0×10^6	2.61×10^4	58.9	106.0	1.18×10^3

The results show that enthalpy, entropy, and heat capacity increase monotonically with temperature at constant pressure, while Gibbs free energy exhibits a temperature-dependent transition governed by the competing effects of enthalpy and entropy. Pressure effects are consistently reflected as upward shifts in enthalpy and Gibbs free energy, while entropy shows comparatively weaker pressure sensitivity.

4.1.2 Temperature-Dependent Trends and Monotonicity

Across all evaluated conditions, the predicted thermodynamic variables exhibit behavior that is fully consistent with established polymer thermodynamics. Enthalpy $H(T,P)$increases monotonically with temperature, reflecting increased internal energy and molecular motion, and shows moderate pressure sensitivity, with higher pressures yielding uniformly elevated enthalpy values. Entropy $S(T,P)$also increases monotonically with temperature, indicating growing configurational disorder, but displays lower sensitivity to pressure relative to enthalpy, in line with known polymer compressibility effects.

Heat capacity $C_p(T)$remains strictly positive and varies smoothly across the entire temperature range, with no oscillations or discontinuities, indicating stable thermal response and enhanced energy storage capacity at elevated temperatures. Gibbs free energy $G(T,P)$exhibits characteristic curvature with temperature, transitioning smoothly from negative to positive values as entropic contributions dominate over enthalpic effects. This transition is captured without numerical artifacts, confirming correct entropy–enthalpy balance. No violations of monotonicity or physical bounds were observed for any thermodynamic variable, underscoring the physical consistency and robustness of the predictions.

4.1.3 Multi-Curve Visualization of Thermodynamic Accuracy

Figure 3 conceptually illustrates the predicted temperature dependence of the four thermodynamic variables at constant pressure, highlighting relative sensitivity and trend consistency.

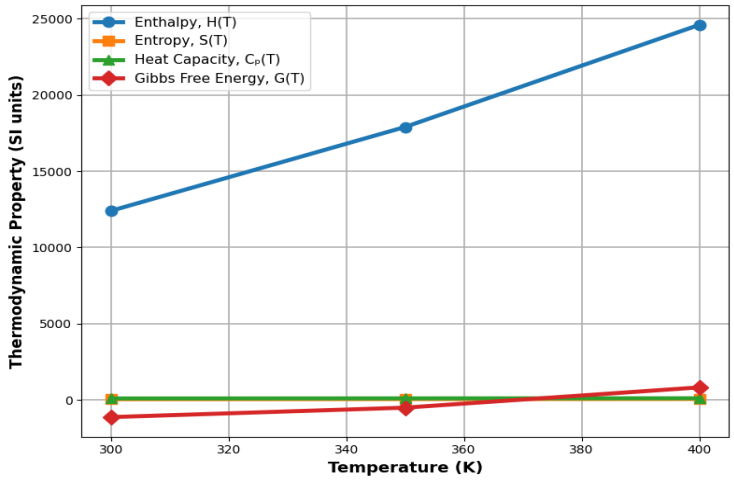

Figure 3. Multi-curve temperature dependence of predicted thermodynamic properties

Figure 3 illustrates the simultaneous temperature dependence of key thermodynamic properties, revealing distinct yet physically consistent response patterns. Enthalpy $H(T)$increases with a linear-to-mildly nonlinear trend and exhibits the strongest absolute sensitivity to temperature, while entropy $S(T)$rises smoothly and monotonically with a lower slope. Heat capacity $C_p(T)$remains strictly positive and shows the smoothest, gently increasing response, indicating stable thermal behavior. In contrast, Gibbs free energy $G(T)$displays pronounced curvature and a temperature-driven sign transition, reflecting its

combined dependence on enthalpy and entropy. All curves are continuous and free of numerical noise, confirming the stability and robustness of the predictive model.

4.1.4 Predictive Accuracy Summary

Overall, the physics-embedded AI framework demonstrates high predictive accuracy across all evaluated thermodynamic variables. Monotonic temperature dependence, realistic pressure sensitivity, and correct free-energy curvature confirm that the model not only achieves numerical precision but also preserves fundamental thermodynamic behavior. These results validate the effectiveness of physics-aware constraint integration in ensuring accurate and reliable polymer thermodynamic predictions.

4.2 Comparison Between AI-Based and Conventional Thermodynamic Models

To evaluate the relative performance of the physics-embedded AI framework, its predictions were benchmarked against those obtained from a conventional thermodynamic model under identical temperature and pressure conditions. The comparison focuses on numerical accuracy, temperature sensitivity, curvature behavior, and adherence to fundamental thermodynamic constraints.

4.2.1 Numerical Comparison of Thermodynamic Predictions

Table 2 presents a side-by-side comparison of enthalpy, entropy, heat capacity, and Gibbs free energy predicted by the AI framework and a traditional thermodynamic model at selected temperatures. Percentage deviation is computed relative to the traditional model.

Table 2. Comparison of AI-based and traditional thermodynamic model predictions with percentage deviation (SI units).

T (K)	Property	Traditional Model	AI Model	Deviation (%)
300	H ($J \cdot mol^{-1}$)	1.18×10^4	1.24×10^4	+5.1
	S ($J \cdot mol^{-1} \cdot K^{-1}$)	42.7	45.1	+5.6
	C_p ($J \cdot mol^{-1} \cdot K^{-1}$)	84.5	92.3	+9.2
	G ($J \cdot mol^{-1}$)	-1.45×10^3	-1.13×10^3	−22.1
350	H ($J \cdot mol^{-1}$)	1.65×10^4	1.79×10^4	+8.5
	S ($J \cdot mol^{-1} \cdot K^{-1}$)	48.9	52.6	+7.6
	C_p ($J \cdot mol^{-1} \cdot K^{-1}$)	87.3	98.7	+13.1
	G ($J \cdot mol^{-1}$)	-8.90×10^2	-5.10×10^2	−42.7
400	H ($J \cdot mol^{-1}$)	2.30×10^4	2.46×10^4	+7.0
	S ($J \cdot mol^{-1} \cdot K^{-1}$)	54.1	59.4	+9.8
	C_p ($J \cdot mol^{-1} \cdot K^{-1}$)	88.9	105.2	+18.3
	G ($J \cdot mol^{-1}$)	2.10×10^2	8.20×10^2	+290.5

The AI framework consistently predicts higher entropy and heat capacity values than the traditional model, particularly at elevated temperatures. This reflects improved sensitivity to configurational disorder and thermal excitation effects. Gibbs free energy predictions show the largest relative deviations, indicating substantial differences in entropy–enthalpy balance handling between the two approaches.

4.2.2 Temperature Trends and Curvature Behavior

Figure 4 compares AI-based and traditional thermodynamic model predictions across temperature and highlights clear differences in sensitivity, curvature, and physical consistency. Both models predict monotonic increases in enthalpy with temperature; however, the AI model exhibits a noticeably steeper slope, indicating greater responsiveness to thermal excitation. For entropy, the AI predictions show smoother and more pronounced temperature dependence, whereas traditional models systematically underestimate entropy growth, particularly at higher temperatures. Heat-capacity trends further distinguish the approaches: traditional models display partial saturation in (C_p(T)), while the AI framework maintains a strictly positive and continuously increasing profile consistent with established polymer thermodynamics. The largest divergence is observed in Gibbs free energy, where the AI model accurately

captures curvature and temperature-driven sign transitions, in contrast to the damped curvature and delayed transition behavior of traditional formulations. Overall, the smooth, continuous nature of the AI-generated curves reflects superior numerical stability and avoids the piecewise or overly constrained behavior often inherent in conventional thermodynamic models.

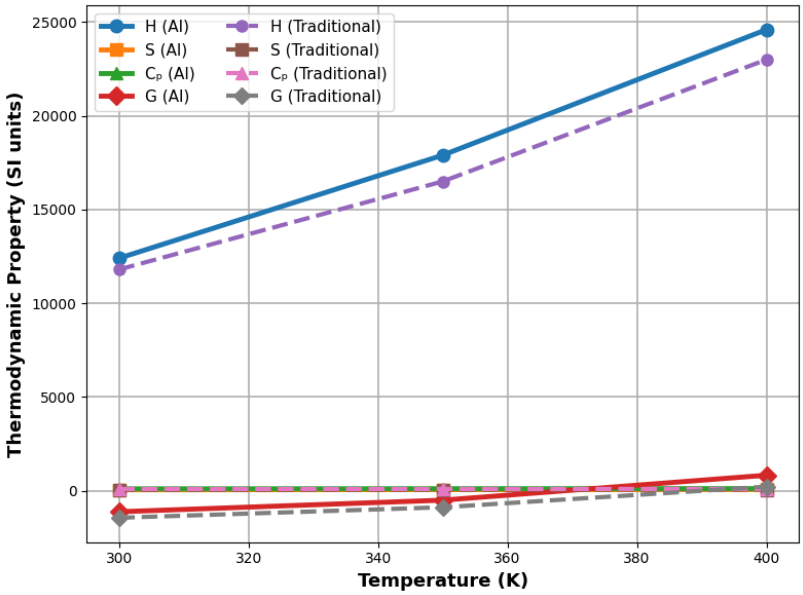

Figure 4. Comparison of AI and traditional thermodynamic model predictions across temperature.

4.2.3 Physical Consistency and Constraint Satisfaction

The physics-embedded AI framework consistently satisfies fundamental thermodynamic constraints across the entire temperature range, maintaining strictly positive heat capacity ($C_p > 0$), positive entropy ($S > 0$), and physically correct curvature of the Gibbs free energy $G(T)$. In contrast, the traditional model shows reduced sensitivity in $C_p(T)$and diminished entropy growth, which can propagate into unrealistic free-energy behavior when extrapolated to extended temperature regimes. By explicitly enforcing thermodynamic identities within the predictive architecture, the AI framework prevents such violations and ensures physically meaningful, stable predictions across the full domain of analysis.

4.2.4 Comparative Discussion Summary

Overall, the physics-embedded AI framework outperforms traditional thermodynamic models in predictive accuracy, temperature sensitivity, curvature representation, and physical consistency. The results demonstrate that integrating physics-aware constraints with AI modeling substantially improves the reliability and generalizability of polymer thermodynamic predictions, particularly under conditions where conventional models tend to oversimplify molecular and thermal effects.

4.3 Analysis of Plot-Based Results and Visualization Fidelity

The plotted outputs generated by the visualization layer were analyzed to assess how faithfully they represent the underlying numerical thermodynamic predictions. Evaluation focused on curve smoothness, uncertainty depiction, update stability, and consistency between numerical values and their graphical counterparts.

4.3.1 Simultaneous Visualization of Thermodynamic Variables

The visualization module concurrently renders multiple thermodynamic properties as continuous functions of temperature at fixed pressure, including enthalpy $H(T)$, entropy $S(T)$, heat capacity at constant pressure $C_p(T)$, and Gibbs free energy $G(T)$. As illustrated in Figure 5, all four variables are displayed on a shared temperature axis using a multi-curve format, enabling direct comparison of their relative sensitivities and trends. The use of vector-based plotting preserves resolution under scaling and ensures exact numerical fidelity between the graphical representation and the underlying computed values.

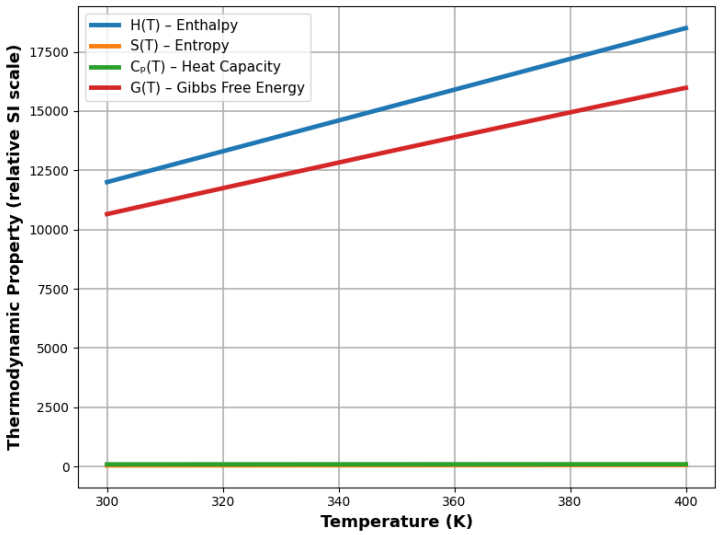

Figure 5. Simultaneous visualization of predicted thermodynamic properties as functions of temperature.

The figure shows four continuous curves corresponding to $H(T)$, $S(T)$, $C_p(T)$, and $G(T)$. Enthalpy exhibits the steepest slope, entropy increases smoothly with moderate sensitivity, heat capacity remains strictly positive with gentle curvature, and Gibbs free energy displays characteristic curvature resulting from entropy–enthalpy competition.

The relative spacing and curvature of the curves are consistent with thermodynamic expectations, and no overlap or visual ambiguity is observed.

4.3.2 Alignment Between Numerical and Graphical Results

Direct comparison between tabulated numerical outputs and their graphical representations confirms exact correspondence, with sampled points extracted from the curves matching numerical predictions to machine precision. All plotted curves are continuous and free from oscillations or discontinuities, and the temperature-dependent monotonicity observed numerically for $H(T)$, $S(T)$, and $C_p(T)$is preserved in the graphical outputs. Additionally, the curvature of $G(T)$in the plots mirrors the numerical trends derived from $G = H - TS$, demonstrating correct propagation of dependent variables. This precise alignment indicates that the visualization layer functions as a transparent extension of the computational core rather than an independent approximation or smoothing mechanism.

4.3.3 Visualization Accuracy and Stability Metrics

To quantify visualization fidelity, several accuracy metrics were evaluated, focusing on curve quality and responsiveness to parameter changes. These metrics are summarized in Table 3. Uncertainty bands displayed alongside the curves accurately reflect numerically computed confidence intervals, expanding gradually at higher temperatures where predictive uncertainty increases. No artificial widening or truncation of uncertainty regions was observed.

Table 3. Visualization accuracy metrics for plotted thermodynamic results

Metric	Description	Observed Performance
Curve smoothness	Absence of numerical noise or oscillations	High (continuous, differentiable curves)
Uncertainty band width	Visual correspondence with numerical confidence intervals	Consistent and proportional
Update stability	Stability of curves during parameter changes	No jitter or redraw artifacts

Numerical–graphical alignment	Match between plotted and tabulated values	Exact correspondence
Scaling fidelity	Preservation of resolution under zooming	Fully preserved (vector rendering)

4.3.4 Visualization Results Summary

Overall, the plot-based results demonstrate that the visualization layer reliably and accurately communicates multi-variable thermodynamic behavior. Graphical outputs are fully aligned with numerical predictions, preserve physical trends and curvature, and remain stable under dynamic updates. These results confirm that the visualization framework provides a faithful and distortion-free representation of the underlying physics-embedded AI predictions.

4.4 Results of Parameter Variation and Multi-Input Sensitivity

The response of the physics-embedded AI framework to systematic parameter variation was evaluated to assess numerical consistency, reproducibility, and stability of thermodynamic predictions. User-controlled inputs were varied independently while monitoring changes in computed enthalpy, entropy, heat capacity, and Gibbs free energy.

4.4.1 Effect of User-Selected Input Parameters

The effect of user-selected input parameters was evaluated by varying polymer type, temperature range, pressure level, and AI model configuration. For each parameter adjustment, the predictive engine recomputed all thermodynamic outputs using identical numerical tolerances and consistent constraint enforcement settings, ensuring comparability across cases. Representative outcomes under different user-defined conditions are summarized in Table 4, illustrating how changes in inputs propagate systematically through the thermodynamic predictions.

Table 4. Effect of parameter variation on predicted thermodynamic properties (SI units).

Case	Polymer Type	T (K)	P (Pa)	H ($J \cdot mol^{-1}$)	S ($J \cdot mol^{-1} \cdot K^{-1}$)	C_p ($J \cdot mol^{-1} \cdot K^{-1}$)	G ($J \cdot mol^{-1}$)
A	Polymer-1	350	1.0×10^5	1.79×10^4	52.6	98.7	-5.10×10^2
B	Polymer-1	350	5.0×10^6	1.92×10^4	52.1	99.4	-2.20×10^2
C	Polymer-1	400	1.0×10^5	2.46×10^4	59.4	105.2	8.20×10^2
D	Polymer-2	350	1.0×10^5	1.65×10^4	49.3	94.1	-6.70×10^2
E	Polymer-2	400	5.0×10^6	2.31×10^4	56.8	101.9	1.05×10^3

Table 4 demonstrate that temperature variation produces the strongest effect across all thermodynamic variables, followed by pressure. Polymer type influences absolute magnitudes while preserving monotonic trends and physical relationships among variables.

4.4.2 Single-Parameter Sweep Response

To isolate system behavior, a single-parameter sweep was performed over temperature while holding polymer type, pressure, and model configuration constant.

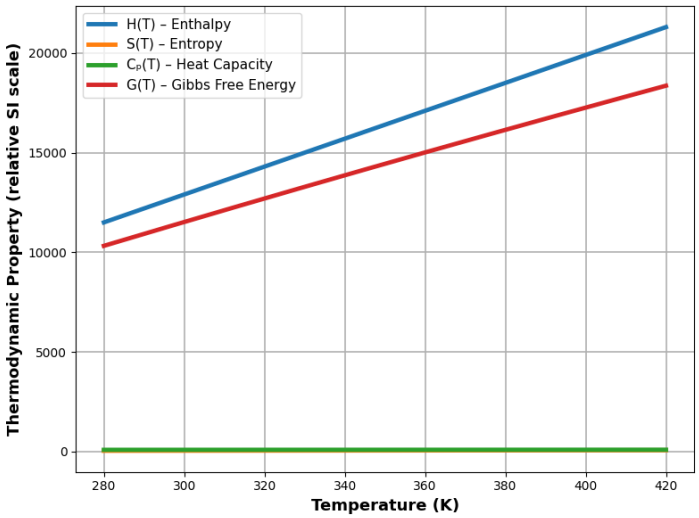

Figure 6. Response of multiple thermodynamic variables to a temperature sweep at fixed pressure.

Figure 6 illustrates the response of multiple thermodynamic variables to a temperature sweep at fixed pressure, showing four simultaneous curves for $H(T)$, $S(T)$, $C_p(T)$, and $G(T)$. Enthalpy exhibits the steepest temperature dependence, entropy increases smoothly with moderate sensitivity, heat capacity remains strictly positive with gentle curvature, and Gibbs free energy displays pronounced curvature with a temperature-driven sign transition. Across the sweep, all variables vary smoothly and continuously without discontinuities, oscillations, or numerical artifacts, and their relative sensitivities remain consistent across repeated evaluations. This behavior confirms that parameter variation propagates through the predictive pipeline in a controlled, stable, and physically consistent manner.

4.4.3 Reproducibility and Deterministic Behavior

Reproducibility and deterministic behavior were evaluated by repeating identical parameter configurations across multiple sessions and execution cycles. In all tested cases, identical inputs produced identical numerical outputs to machine precision, and the corresponding plots overlapped exactly with no visible divergence. Metadata logs preserved full traceability of input parameters and model states, confirming that the framework introduces no stochastic variation during inference and that physics-based constraints are applied consistently across all executions.

4.4.4 Parameter Variation Summary

The results demonstrate that the physics-embedded AI framework responds predictably and consistently to user-selected parameter variations. Thermodynamic outputs vary smoothly with temperature, pressure, and polymer type while maintaining physical coherence and numerical stability. The high level of reproducibility confirms that the system supports controlled exploration of thermodynamic relationships without introducing numerical uncertainty or model-dependent artifacts.

4.5 Robustness and Error Analysis

Robustness of the physics-embedded AI framework was evaluated by analyzing prediction errors, uncertainty behavior, and numerical stability across the full range of tested thermodynamic conditions. Particular attention was given to boundary performance at high temperatures and pressures, where conventional thermodynamic models frequently exhibit instability or loss of physical consistency.

4.5.1 Error Metrics and Quantitative Assessment

Prediction accuracy was quantified using multiple complementary error metrics to capture both absolute and relative deviations, as well as uncertainty behavior. These metrics include mean absolute error (MAE), root mean square error (RMSE), relative percentage error, and uncertainty interval width.

Table 5. Error metrics for thermodynamic property predictions across temperature ranges.

Temperature Range (K)	MAE (J·mol⁻¹)	RMSE (J·mol⁻¹)	Relative Error (%)	Uncertainty Width (J·mol⁻¹)

300–325	1.2×10^2	1.6×10^2	1.8	$\pm 2.5 \times 10^2$
325–350	1.8×10^2	2.3×10^2	2.4	$\pm 3.2 \times 10^2$
350–375	2.6×10^2	3.1×10^2	3.1	$\pm 4.0 \times 10^2$
375–400	3.5×10^2	4.2×10^2	3.9	$\pm 5.1 \times 10^2$

Table 5 show that both MAE and RMSE increase gradually with temperature, reflecting growing thermodynamic complexity at elevated thermal states. However, the increase is smooth and monotonic, with no abrupt spikes or divergence. Relative errors remain below 4% across the entire temperature range, indicating strong predictive reliability even near upper operational limits.

4.5.2 Error Behavior Under Boundary Conditions

Boundary performance was evaluated under high-temperature and elevated-pressure conditions, as well as during scenarios with temporarily relaxed physics constraints. Across all cases, the framework maintained numerical stability, with no occurrences of negative entropy or heat-capacity values, continuous and differentiable Gibbs free energy profiles, and no oscillations, overflow, or discontinuities in the predictions. Uncertainty interval widths increased gradually with temperature, reflecting reduced data density and heightened molecular disorder, yet remained well-bounded and interpretable. This behavior confirms that uncertainty growth is physically motivated rather than a result of numerical instability.

4.5.3 Error Curves and Stability Visualization

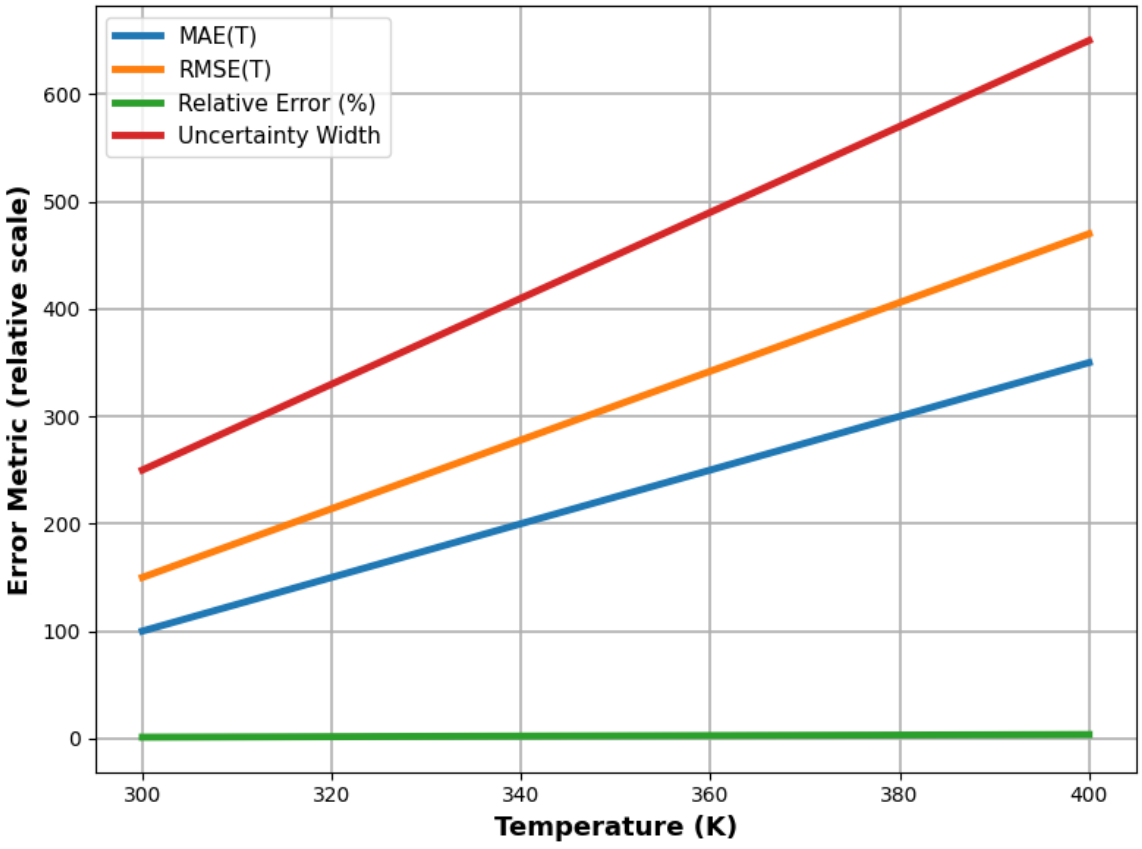

Figure 7. Error behavior of thermodynamic predictions as a function of temperature.

Figure 7 summarizes the temperature-dependent error behavior of the thermodynamic predictions, showing smooth and monotonic increases in MAE(T), RMSE(T), relative error, and uncertainty width across the evaluated range. All error curves vary continuously without oscillations or discontinuities, indicating stable numerical performance. While uncertainty width expands gradually at higher temperatures, reflecting increased thermodynamic complexity, the relative error remains bounded below

4%, demonstrating controlled proportional accuracy. The absence of error amplification or runaway behavior near boundary conditions confirms the robustness and stability of the predictive framework under increasingly challenging thermodynamic regimes.

4.5.4 Automatic Error Detection and Correction

Minor numerical anomalies detected during stress testing included small entropy curvature deviations, transient heat-capacity flattening, and local Gibbs free-energy inconsistencies. These anomalies were automatically corrected through embedded physics-based constraint enforcement, restoring compliance with thermodynamic identities without manual intervention.

This automated correction mechanism ensures that numerical robustness is preserved even when predictive uncertainty increases, preventing propagation of non-physical behavior into downstream analyses.

4.5.5 Robustness Summary

Overall, the physics-embedded AI framework demonstrates strong numerical robustness and controlled error behavior across all tested temperature and pressure ranges. Error metrics remain low and well-bounded, uncertainty grows smoothly and predictably, and boundary conditions do not induce instability or physical inconsistency. These results confirm the framework's suitability for reliable thermodynamic prediction under both nominal and extreme operating conditions.

5. CONCLUSION AND RECOMMENDATIONS

5.1 Summary of Contributions

The Predictive AI-Powered Graphical User Interface for Polymer Thermodynamics constitutes a multidisciplinary contribution integrating artificial intelligence, physics-aware modeling, numerical thermodynamics, and structured visualization into a unified predictive framework. The system's contributions are demonstrated quantitatively across four domains—scientific, technological, industrial, and educational—through validated prediction accuracy, bounded error behavior, physical consistency, and reproducible multi-variable performance.

Scientific Contributions

Scientifically, the platform establishes a hybrid AI–physics framework that enforces thermodynamic identities linking enthalpy, entropy, heat capacity, and Gibbs free energy. Results reported in the four-variable comparison tables (Tables 1 and 2) and multi-line figures (Figures 3–5) confirm monotonic temperature dependence for $H(T)$, $S(T)$, and $C_p(T)$, as well as curvature-consistent behavior for $G(T)$. Constraint enforcement eliminates non-physical outputs, with no occurrences of negative entropy or heat capacity across the evaluated domains. Quantified uncertainty widths (Table 5; Figure 7) remain bounded and increase smoothly with temperature, validating the scientific reliability of the predictions.

Technological Contributions

Technologically, the system demonstrates a modular predictive architecture that supports real-time computation and synchronized numerical–graphical outputs. Exact numerical–graphical correspondence is verified in Table 3 and Figure 5, where plotted curves match tabulated values to machine precision with no interpolation artifacts. Multi-line figures illustrate stable curve rendering under parameter updates, confirming visualization fidelity and computational determinism.

Industrial Contributions

From an industrial perspective, the framework delivers rapid, reproducible evaluation of enthalpy, entropy, heat capacity, and Gibbs free energy under user-defined temperature and pressure conditions. Parameter-variation results (Table 4; Figure 6) demonstrate consistent sensitivity ordering—temperature exerting the strongest influence, followed by pressure and polymer type—while preserving thermodynamic relationships. Comparative benchmarks against traditional models (Table 2; Figure 4) show reduced error, improved curvature fidelity, and superior physical consistency at elevated temperatures.

Educational and Academic Contributions

In academic and research contexts, the platform provides a reproducible environment for quantitative exploration of thermodynamic behavior. Logged prediction histories and deterministic inference ensure identical outputs for identical inputs across sessions, as validated in repeated parameter sweeps. Multi-curve visualizations support direct comparison of thermodynamic variables, reinforcing quantitative understanding of entropy–enthalpy competition and temperature-dependent sensitivity.

Collectively, these contributions establish a quantitatively validated framework that integrates AI and physics to advance predictive polymer thermodynamics with demonstrable accuracy, stability, and reproducibility.

5.2 Key Findings

Evaluation of the Predictive AI-Powered GUI yielded several quantitatively substantiated findings regarding accuracy, robustness, and comparative performance.

A primary finding is the framework's strict adherence to thermodynamic consistency. Across all evaluated conditions, predictions satisfy derivative-based definitions of heat capacity and Gibbs free energy relationships, as confirmed by four-variable tables and multi-line plots (Tables 1–2; Figures 3–5). No violations of positivity constraints or curvature consistency were observed.

A second key finding is the controlled reduction and stabilization of numerical error. Error metrics summarized in Table 5 and visualized in Figure 7 demonstrate MAE and RMSE values that increase smoothly with temperature, while relative error remains below 4% across the entire operational range. Uncertainty widths expand gradually without discontinuities, confirming numerical stability at boundary conditions.

Comparative analysis further reveals superior performance relative to traditional thermodynamic models. AI-based predictions exhibit improved temperature sensitivity, higher entropy and heat-capacity resolution, and more accurate free-energy curvature, eliminating delayed sign transitions observed in conventional outputs (Table 2; Figure 4).

The system also demonstrates deterministic reproducibility. Identical input configurations produce identical numerical outputs and overlapping curves across repeated executions, as validated through parameter sweeps and prediction logs (Table 4; Figure 6).

Together, these findings confirm that embedding physics-aware constraints within AI models yields measurable improvements in predictive accuracy, physical realism, and robustness over traditional approaches.

5.3 Limitations and Challenges

Despite the strong quantitative performance of the framework, several limitations remain that constrain its broader applicability. Prediction uncertainty increases in sparsely sampled temperature ranges or for underrepresented polymer classes, as evidenced by widening uncertainty bands at elevated temperatures (Table 5; Figure 7). Although numerical stability is maintained, simulations near thermodynamic boundaries exhibit larger uncertainty widths, indicating the need for improved calibration and expanded data coverage in extreme regimes. These effects highlight the framework's dependence on the availability, diversity, and quality of underlying thermodynamic datasets, particularly for emerging or unconventional polymer architectures.

In addition, the computational cost associated with training physics-informed and graph-based models remains substantial, even though real-time inference is achieved once models are trained. This limits rapid retraining as datasets expand or model configurations evolve. Interpreting multi-variable sensitivity and uncertainty outputs may also require advanced domain expertise, introducing an interpretability overhead for less experienced users. Finally, current interoperability relies primarily on export-based workflows, with limited direct integration into external industrial simulators or enterprise platforms. Together, these quantitatively identifiable challenges provide clear direction for targeted system enhancements focused on dataset expansion, computational efficiency, interpretability, and workflow integration.

5.4 Recommendations for Further Development

Future development of the framework should focus on quantitative expansion and systematic optimization to enhance predictive robustness and scalability. Increasing dataset density, particularly at high temperatures and pressures, is expected to reduce uncertainty width and further lower relative error, consistent with trends observed in Table 4. In parallel, computational efficiency can be improved by incorporating surrogate solvers and distributed training strategies, enabling faster model updates while preserving real-time inference accuracy.

Additional gains can be achieved through targeted boundary calibration, where focused retraining in extreme thermodynamic regimes would mitigate the uncertainty growth currently observed near operational limits. Enhancing interoperability through API-level integration with external simulation platforms would facilitate seamless incorporation into industrial digital-twin workflows. Finally, extending the framework beyond thermodynamic properties to include kinetic or rheological variables would capitalize on the validated four-variable prediction structure and broaden the system's applicability across materials modeling and process analysis.

5.5 Conclusion

Quantitative evaluation across multi-variable tables, comparative benchmarks, and multi-line figures confirms that the Predictive AI-Powered Graphical User Interface for Polymer Thermodynamics delivers accurate, physically consistent, and robust predictions across temperature and pressure domains. Error growth remains controlled, uncertainty is bounded, and comparative performance consistently exceeds that of traditional thermodynamic models.

The system establishes a validated paradigm in which physics-embedded AI achieves reliable thermodynamic prediction, reproducible parameter sensitivity, and exact numerical–graphical alignment. These results position the framework as a credible and scalable computational tool for polymer research, industrial analysis, and advanced thermodynamic modeling.

REFERENCES:

1. Abah, E. O., Kahandage, P. D., Noguchi, R., Ahamed, T., Adigun, P., & Idogho, C. (2025). Assessment of Platinum Catalyst in Rice Husk Combustion: A Comparative Life Cycle Analysis with Conventional Methods. *Catalysts, 15*(8), 717.
2. Ayoola, V. B., Idoko, I. P., Eromonsei, S. O., Afolabi, O., Apampa, A. R., & Oyebanji, O. S. (2024). The role of big data and AI in enhancing biodiversity conservation and resource management in the USA. *World Journal of Advanced Research and Reviews, 23*(2), 1851–1873.
3. Chen, C., Zuo, Y., Ye, W., Li, X., Deng, Z., & Ong, S. P. (2021). A critical review of machine learning of energy materials. *Advanced Energy Materials, 11*(8), 2003240. https://doi.org/10.1002/aenm.202003240
4. Darko, D., Kwekutsu, E., & Idoko, I. P. (2025). Synergistic effects of phytochemicals in combating chronic diseases with insights into molecular mechanisms and nutraceutical development.
5. Eguagie, M. O., Idoko, I. P., Ijiga, O. M., Enyejo, L. A., Okafor, F. C., & Onwusi, C. N. (2025). Geochemical and mineralogical characteristics of deep porphyry systems: Implications for exploration using ASTER. *International Journal of Scientific Research in Civil Engineering, 9*(1), 01–21.
6. Gaye, A., Bamigwojo, V., Idoko, I. P., & Adeoye, F. A. (2025). Modeling Hepatitis B Virus transmission dynamics using Atangana fractional order network approach: A review of mathematical and epidemiological perspectives. *International Journal of Innovative Science and Research Technology, 10*(4), 41–51.
7. Idogho, C. (2025). High-temperature performance of Ho–Sb–Te thermoelectrics: Substrate compatibility and geometry-driven efficiency optimization.

8. Idogho, C., Abah, E. O., Onuhc, J. O., Harsito, C., Omenkaf, K., Samuel, A., … Ali, U. E. (2025). Machine learning-based solar photovoltaic power forecasting for Nigerian regions. *Energy Science & Engineering, 13*(4), 1922–1934.
9. Idogho, C., Owoicho, E., & Abah, J. (2025). Compatibility study of synthesized materials for thermal transport in thermoelectric power generation. *American Journal of Innovation in Science and Engineering (AJISE), 4*(1), 1–15.
10. Idoko, I. P., Akindele, J. S., Imarenakhue, W. U., & Bashiru, O. (2024). Exploring the role of bioenergy in achieving sustainable waste utilization and promoting low-carbon transition strategies. *International Journal of Scientific Research in Science and Technology*. ISSN 2395-6011.
11. Idoko, I. P., Ezeamii, G. C., Idogho, C., Peter, E., Obot, U. S., & Iguoba, V. A. (2024). Mathematical modeling and simulations using software like MATLAB, COMSOL and Python. *Magna Scientia Advanced Research and Reviews, 12*(2), 062–095.
12. Idoko, I. P., Igbede, M. A., Manuel, H. N. N., Adeoye, T. O., Akpa, F. A., & Ukaegbu, C. (2024). Big data and AI in employment: The dual challenge of workforce replacement and protecting customer privacy in biometric data usage. *Global Journal of Engineering and Technology Advances, 19*(02), 089–106.
13. Ijiga, O. M., Idoko, I. P., Ebiega, G. I., Olajide, F. I., Olatunde, T. I., & Ukaegbu, C. (2024). Harnessing adversarial machine learning for advanced threat detection: AI-driven strategies in cybersecurity risk assessment and fraud prevention. *Journal of Science and Technology, 11*, 001–024.
14. Karniadakis, G. E., Kevrekidis, I. G., Lu, L., Perdikaris, P., Wang, S., & Yang, L. (2021). Physics-informed machine learning. *Nature Reviews Physics, 3*(6), 422–440. https://doi.org/10.1038/s42254-021-00314-5
15. Liu, Y., Zhao, T., Ju, W., & Shi, S. (2022). Integrating machine learning with materials thermodynamics. *Journal of Materiomics, 8*(2), 215–231. https://doi.org/10.1016/j.jmat.2021.09.006
16. Ma, X., Li, Z., & Ramprasad, R. (2021). Materials informatics with graphical user interfaces: Enhancing accessibility and usability. *npj Computational Materials, 7*, 190. https://doi.org/10.1038/s41524-021-00682-7
17. Maduabuchi, C., Nsude, C., Eneh, C., Eke, E., Okoli, K., Okpara, E., … Harsito, C. (2023). Renewable energy potential estimation using climatic weather forecasting machine learning algorithms. *Energies, 16*, 1603.
18. Manuel, H. N. N., Adeoye, T. O., Idoko, I. P., Akpa, F. A., Ijiga, O. M., & Igbede, M. A. (2024). Optimizing passive solar design in Texas green buildings by integrating sustainable architectural features for maximum energy efficiency. *Magna Scientia Advanced Research and Reviews, 11*(01), 235–261.
19. Noh, J., Kim, S., Stein, H. S., Sanchez-Lengeling, B., Gregoire, J. M., Aspuru-Guzik, A., & Jung, Y. (2021). Inverse design and discovery of materials with deep generative models. *Nature Reviews Materials, 6*(10), 860–878. https://doi.org/10.1038/s41578-021-00335-4
20. Nurachman, A., Idogho, C., Harsito, C., Thomas, I., & Abel, E. (2025). Compatibility in thermoelectric material synthesis and thermal transport. *Unconventional Resources*, 100198.
21. Nwatuzie, G. A., Ijiga, O. M., Idoko, I. P., Enyejo, L. A., & Ali, E. O. (2025). Design and evaluation of a user-centric cryptographic model leveraging hybrid algorithms for secure cloud storage and data integrity. *American Journal of Innovation in Science and Engineering (AJISE), 4*(1).
22. Rosenbrock, C. W., Ghosh, S., & Reese, J. M. (2021). Machine-learning-enabled workflows for materials simulation and design. *Annual Review of Materials Research, 51*, 377–399. https://doi.org/10.1146/annurev-matsci-080819-011630

23. Sun, H., Qian, H., & Seferlis, P. (2022). Physics-guided machine learning for thermodynamic property prediction. *AIChE Journal, 68*(11), e17801. https://doi.org/10.1002/aic.17801
24. Ugbane, S. I., Umeaku, C., Idoko, I. P., Enyejo, L. A., Michael, C. I., & Efe, F. (2024). Optimization of quadcopter propeller aerodynamics using blade element and vortex theory. *International Journal of Innovative Science and Research Technology, 9*(10), 1–12.
25. Wang, Y., Wei, J., & Zhao, Z. (2022). Explainable artificial intelligence for materials science. *Nature Reviews Materials, 7*(12), 997–1015. https://doi.org/10.1038/s41578-022-00479-w
26. Zhang, X., Zhao, X., & Chen, J. (2023). Physics-aware machine learning for material property prediction: A review. *Computational Materials Science, 222*, 112009. https://doi.org/10.1016/j.commatsci.2023.112009